MICROVASCULAR RESEARCH 47, 293–307 (1994)

Microvascular Architecture within the Pig Kidney Cortex

L. X. XU,* K. R. HOLMES,†‡ B. MOORE,† M. M. CHEN,§ AND H. ARKIN‖

*Department of Applied Sciences, The College of Staten Island, Staten Island, New York 10301, †Department of Veterinary Biosciences, ‡Bioengineering Faculty, University of Illinois, Urbana, Illinois 61801; §Department of Mechanical Engineering, University of Michigan, Ann Arbor, Michigan 48109, and ‖The National Institute for Building Research, Technion, Haifa 32000, Israel

Received April 5, 1993

Corrosion casts of the plastic (Mercox CI-2B) filled pig kidney cortex vasculature were sliced either parallel or perpendicular to the kidney surface. Scanning electron microscopy photographs were taken of the casts. Montages of the photographs were analyzed using a digitizing tablet and microcomputer-based software. For vessels having diameters larger than 0.05 mm, their sizes, numbers per unit area, and branching patterns were studied with respect to the kidney cortex depth. Vascular branching diameters and angles within the cortex compare favorably with those reported for other major vascular systems. The microvascular dimensions and densities were used to predict the average blood flow velocity within the kidney cortex. It is expected that the results will facilitate a better insight into the contribution of flowing blood to the heat transfer process in perfused tissues.

INTRODUCTION

The distribution of the major vessels within the kidney is well understood, and a system of nomenclature for these vessels has been established (Kriz and Bankir, 1988). However, relatively little attention has been given to the detail of the vascular architecture for vessels whose diameter lies between that of afferent (or efferent) arteriole and the arcuate vessel.

Blood vessels with diameters in the range of approximately 0.05 and 0.5 mm typically can not be seen with the unaided eye. Although vessels in this size range are generally considered too large to be involved in vascular transport, they are receiving attention in the study of tissue heat transfer (Baish *et al.*, 1986a,b; Chato, 1991; Chen and Holmes, 1980; Lemons *et al.*, 1987; Weinbaum *et al.*, 1984). We chose to study the pig kidney because its anatomy is similar to that of the human kidney, the vascular architecture is well organized, and it is being used with increasing frequency in tissue heat transfer studies (Benkeser *et al.*, 1990; Umemura *et al.* 1992). This report provides a quantitative analysis of blood vessels within the pig kidney cortex with lumen diameters $\geq$0.05 mm.

0026-2862/94 $6.00

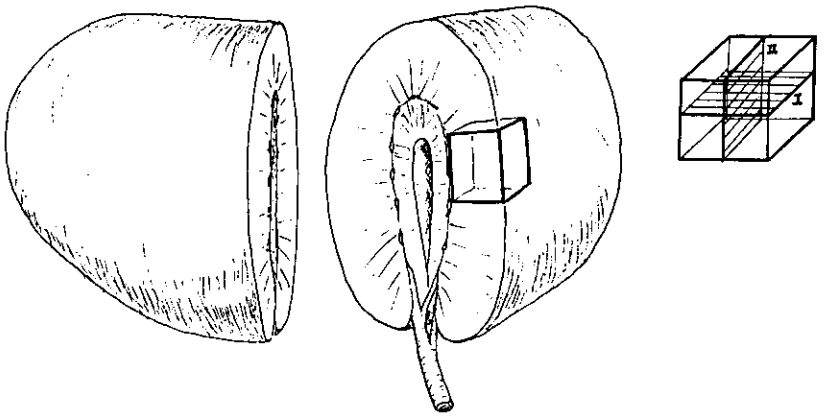

FIG. 1. Schematic drawing of slices cut from a pig kidney cortex vascular cast. I and II denote the directions of cutting to obtain cross and longitudinal sections, respectively.

MATERIALS AND METHODS

We used two female pigs (one Yorkshire and one Duroc) weighing approximately 90 kg each. Pigs were killed with a captive bolt gun. Kidneys were quickly removed through a midventral abdominal incision. Each kidney was grossly similar in appearance (see Fig. 1), measured approximately 15 × 7 × 4 cm, and weighed about 200 g. A standard casting method (Moore *et al.,* 1992) was used to fill the blood vessels with a low-viscosity blue methylmethacrylate plastic (Mercox CL-2B). After injection, the kidneys were wrapped with plastic wrap and left at room temperature for approximately 4 hr to complete the polymerization process. As illustrated in Fig. 1, several blocks of the cortex (approx. 1 cm × 1 cm × cortex thickness) were cut from each kidney. Tissue blocks were taken from a region where the surface of the kidney was very nearly flat, allowing the cross-sectional cuts to be made essentially parallel to the surface. Each block was cut into slices either parallel (cross-sectional) or perpendicular (longitudinal; full cortex thickness) to the kidney surface. All slices were corroded in a solution of warm (50°C) saturated KOH and methanol (80%/20% on volume bases). After 48–72 hr of corrosion, the casts were carefully rinsed in distilled water for several days, frozen in distilled water, and subsequently freeze–dried using a standard method (Moore *et al.,* 1992). The dried slices of vascular casts were prepared for SEM (ISI DS-130 or ISI-40; 5 kV accelerating voltage) by sputter coating with gold-palladium and mounting on 1-⅛″ aluminum stubs.

Low magnification views of a typical cross-sectional and longitudinal cut through the vascular cast are shown in Fig. 2. Twenty to 30 SEM photographs (at about 30× magnification) were taken in a raster fashion to construct a complete montage of each cross-sectional slice. All blood vessel casts with diameters ≥0.05 mm in the montage at different cortex depths were measured and counted using a digitizing tablet and commercial software (SigmaScan; Jandel Scientific). The particular arrangement of these blood vessels within the kidney cortex was such that, with cross-sectional cuts, the vessel casts were cut nearly perpendicular to their long axis. Thus, in many cases, the cut surface was circular and a single mea-

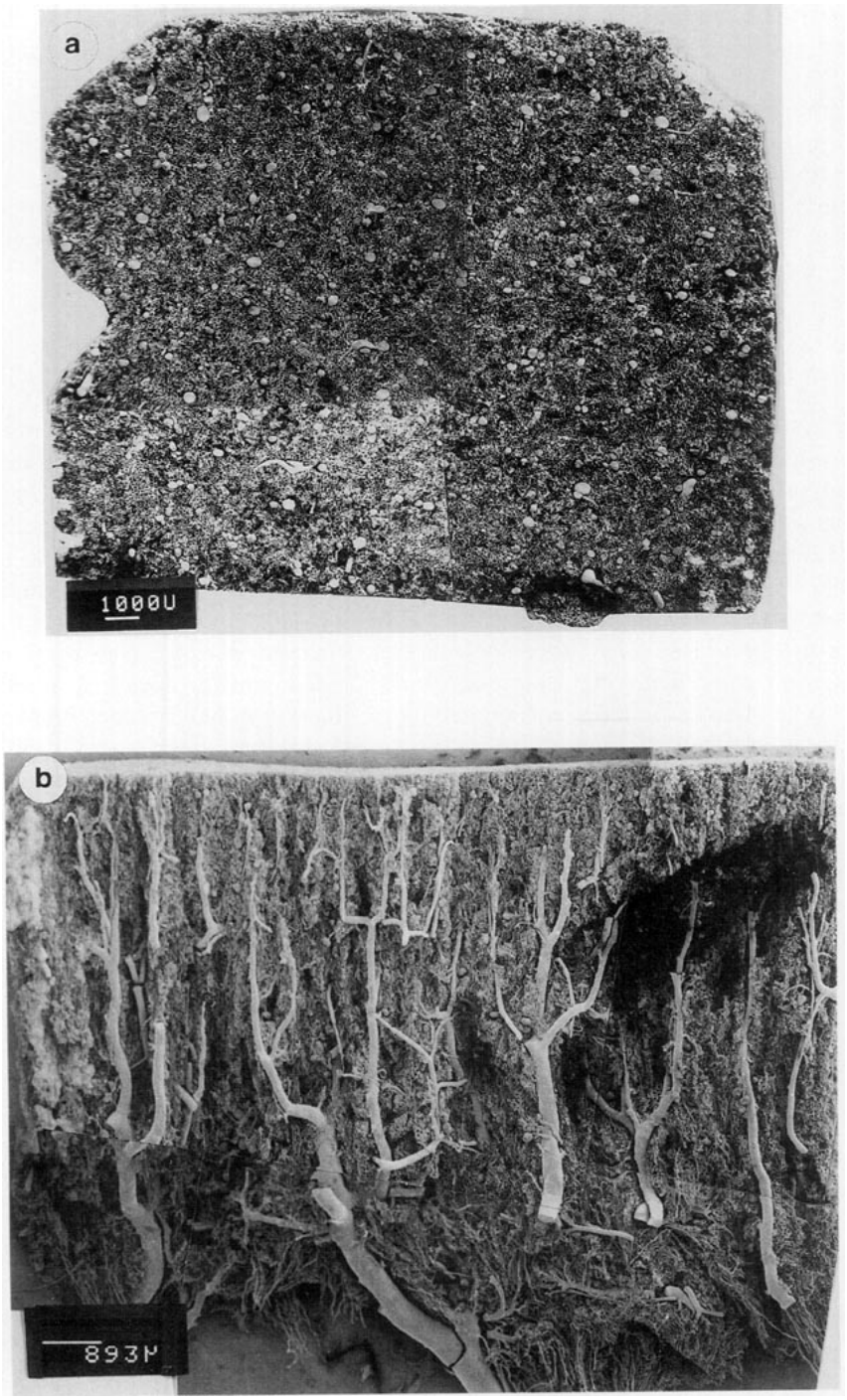

FIG. 2. SEM photographs of typical cross-sectional (a) and longitudinal (b) slices from a pig kidney cortex vascular cast.

surement revealed its diameter. In other instances, however, the cut surfaces were not perfectly round due at least in part to the normal arrangement of the surrounding tissue that existed at the time of plastic injection. In these cases, both the wide and the narrow dimensions were measured and the average was used to represent the cast diameter.

Montages of the longitudinal slices were made in a manner similar to those for the cross-sectional slices. The digitizing tablet and software was used to measure vascular branching locations, as well as parent and daughter diameters within the cortex. Vessel branching patterns were obtained from 125 digitized vessel bifurcations on five different longitudinal montages.

RESULTS AND DISCUSSION

Because of the similarity in shape, overall dimension, and weight, data obtained from the kidneys of both pigs were considered together for subsequent analysis. Although the term "blood vessel" or "vessel" has been used throughout this report, it is pertinent to note that the measurements made of an individual vessel cast reflects the internal (lumen) dimension of the vessel at the time the plastic injection material hardened. The cortex was found to vary somewhat in thickness from region to region. Therefore, measurements of depth within a given tissue block are presented as a percentage (cortex fraction, X_j) of the respective full-thickness cortex. Thus, for example, X_j = 0.0, 0.5, or 1.0 represents the cortex surface, mid-cortex, or the corticomedullary junction (CMJ), respectively.

Table 1 presents the number of vessels ($\geq$0.05 mm diameter per mm^2 of tissue seen in cross-sectional SEM montages made at 17 depths within the cortex. For purposes of analysis, vessels were grouped into 10 ranges with an interval of 0.05 mm. Since arteries could not be distinguished from veins in the SEM mongates, the number in each range includes both arteries and veins.

Data presented in Table 1 indicate that the outer approximately one-third of the pig kidney cortex ($0.0 < X_j < 0.35$) is devoid of vessels >0.3 mm in diameter. Approximately 90% of all the vessels within this part of the cortex have diameters less than 0.15 mm. In the middle portion of the cortex ($0.35 < X_j < 0.65$), Table 1 shows that vessels with diameters in the range of 0.05 to 0.15 mm were distributed rather uniformly throughout although they are fewer in number (33.5 $\pm$ 12.2 per cm^2; mean $\pm$ SD, n = 12) compared to the outer portion (106.2 $\pm$ 49.3 per cm^2; mean $\pm$ SD, n = 20). Further, vessels with lumens >0.3 mm become more numerous with increasing X_j. Proceeding deeper into the inner portion of the cortex ($0.65 < X_j < 1.0$), vessels having diameters <0.25 mm are seen less frequently, whereas larger vessels continued to increase in number as the CMJ is approached. The three-dimensional surface seen in Fig. 3 incorporates data presented in Table 1 to illustrate the relationship between the number of vessels per 100 mm^2 observed within selected diameter ranges at various cortex locations.

When all of the blood vessels ($d \geq 0.05$ mm) were considered, the total cross-sectional area occupied by blood vessels per mm^2 tissue was found to increase with the cortex depth (see Table 1). A linear relationship between the vessel area fraction (VAF) and the cortex fraction is demonstrated in Fig. 4. The total vessel number density (TVND) decreases exponentially with X_j (see Fig. 5). A similar

TABLE 1

NUMBER OF BLOOD VESSELS WITHIN 10 DIAMETER RANGES COUNTED PER mm² OF CROSS-SECTIONAL CORTEX AREA AND THE CORRESPONDING TOTAL VESSEL AREAS AT 17 DIFFERENT CORTEX FRACTIONS

Cortex fraction (X_j)	Vessell number density (VND; No./mm²) within a diameter range (mm)										Total vessel number density (TVND; No./mm²)	Total vessel area per mm² tissue area (VAF; mm²/mm²)
	0.05–0.1	0.1–0.15	0.15–0.2	0.2–0.25	0.25–0.3	0.3–0.35	0.35–0.4	0.4–0.45	0.45–0.5	>0.5		
0.10	2.174	0.669	0.031	0	0	0	0	0	0	0	2.874	0.019
0.12	1.895	0.960	0.050	0	0	0	0	0	0	0	2.905	0.023
0.23	0.658	1.118	0.424	0.051	0.007	0	0	0	0	0	2.258	0.028
0.23	0.827	1.251	0.273	0.022	0	0	0	0	0	0	2.373	0.028
0.29	0.805	0.860	0.302	0.055	0.009	0	0	0	0	0	2.031	0.025
0.33	0.639	0.888	0.355	0.018	0	0	0	0	0	0	1.900	0.024
0.34	0.450	0.654	0.491	0.194	0.061	0.020	0	0	0	0	1.870	0.037
0.36	0.353	0.359	0.237	0.168	0.093	0.029	0.006	0	0	0	1.245	0.027
0.41	0.276	0.184	0.150	0.127	0.104	0.035	0.069	0.023	0	0	0.968	0.033
0.43	0.381	0.444	0.451	0.204	0.078	0.007	0	0	0	0	1.565	0.032
0.50	0.356	0.374	0.283	0.163	0.078	0.006	0	0.006	0	0	1.266	0.027
0.50	0.406	0.244	0.111	0.089	0.066	0.022	0.037	0.015	0.007	0.015	1.012	0.026
0.54	0.425	0.272	0.187	0.068	0.060	0.068	0.009	0.017	0.017	0	1.123	0.028
0.54	0.436	0.232	0.159	0.073	0.041	0.023	0.023	0.018	0.014	0.009	1.028	0.026
0.62	0.183	0.191	0.104	0.157	0.104	0.078	0.061	0	0	0	0.878	0.031
0.65	0.324	0.148	0.095	0.057	0.048	0.048	0.043	0.024	0.019	0.033	0.839	0.034
0.68	0.332	0.146	0.053	0.033	0.100	0.080	0.020	0.046	0	0.033	0.843	0.038
0.68	0.387	0.209	0.108	0.101	0.070	0.077	0.031	0.054	0.023	0	1.060	0.038
0.75	0.152	0.168	0.163	0.065	0.087	0.043	0.027	0.016	0.005	0.005	0.731	0.026
0.85	0.170	0.164	0.080	0.057	0.045	0.045	0.057	0.028	0.023	0.023	0.691	0.034
1.0	0.112	0.112	0.056	0	0	0.028	0	0.028	0	0.140	0.476	0.052
1.0	0.288	0.144	0.086	0.058	0.029	0.058	0.029	0	0	0.086	0.778	0.042

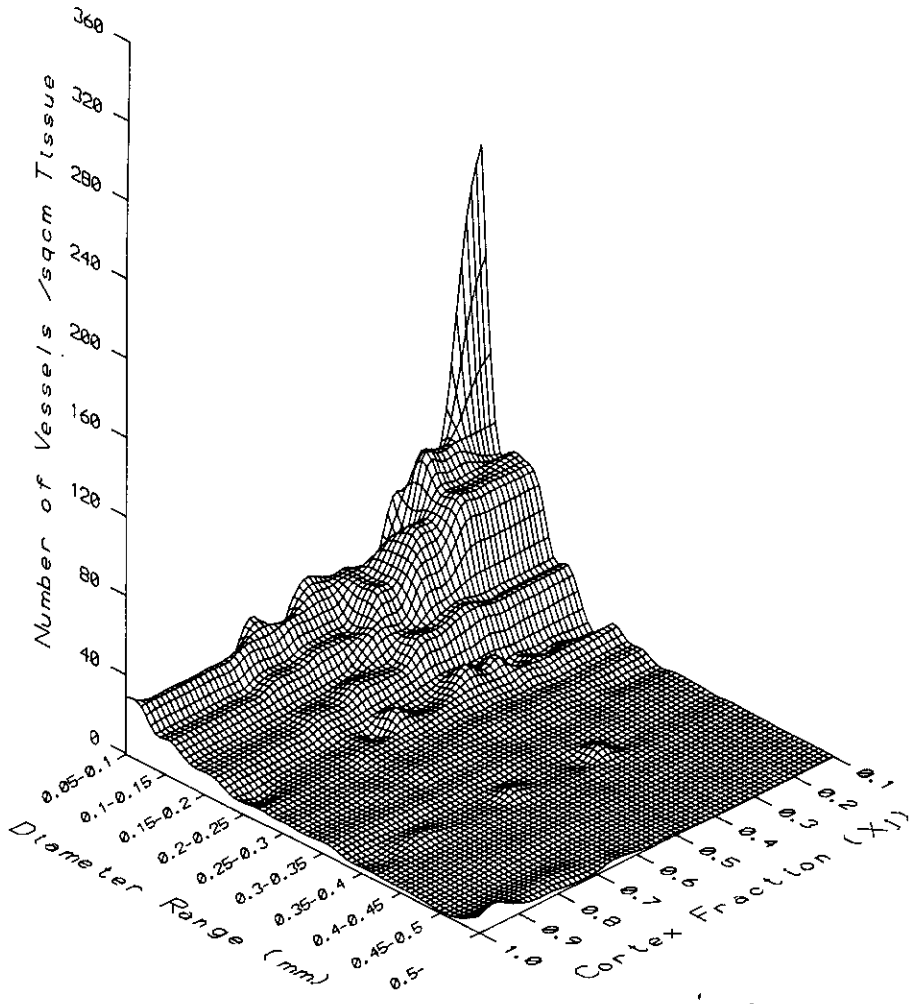

FIG. 3. A three-dimensional view for the number of vessels per 100 mm^2 as a function of the cortex fraction and the vessel size.

relationship has been reported for the vascular branching pattern in the rabbit thigh muscle (Dagan *et al.*, 1986).

Paired vessels have the potential to facilitate countercurrent tissue heat and mass exchange. Table 2 reports the number of paired vessels found in cross-sectional montages at several cortex depths. Vessels were considered to be paired when their juxtaposed surfaces were separated by no more than the dimension of the largest diameter of the two vessels. Based on this criteria, however, it is possible to count two closely spaced branches from the same parent vessel as paired vessels with the result that the actual numbers of paired vessels per unit area might be somewhat less than those shown in Table 2. Based on our analysis of the vascular architecture using longitudinal cuts through the cortex (to be described later), we estimate that there is less than 10% error in these values. Comparing the total number of vessels having diameter $\geq$0.05 mm in Table 2 with that in Table 1, one can find that some counts are slightly different at

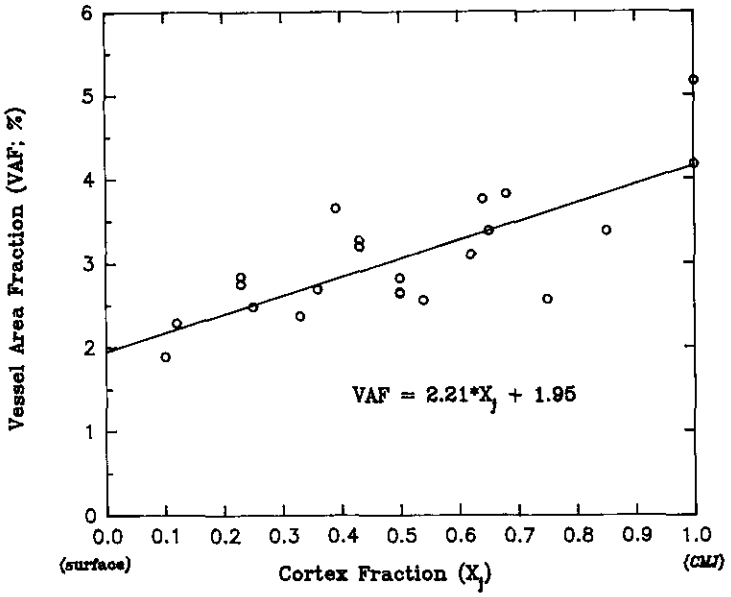

FIG. 4. The cross-sectional vessel area fraction for vessels having diameters ≥0.05 mm vs the cortex fraction. A linear regression of the measured data is shown by the solid line.

corresponding cortex fractions. We attribute the differences to experimental errors caused by two individuals who made measurements at different times. Analysis presented in Fig. 6 suggests that a linear relationship exists between the percentage of vessels which are paired and the cortex fraction; paired vessels occur with

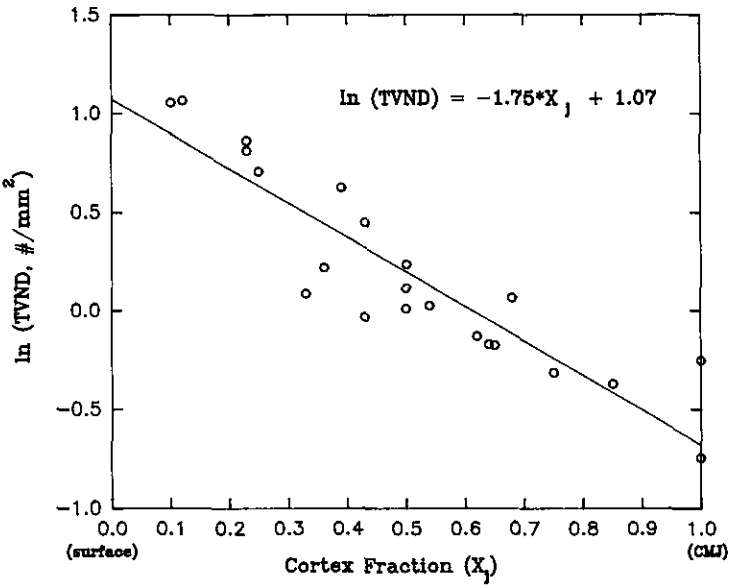

FIG. 5. Total vessel number density for vessels having diameters ≥0.05 mm presented as a function of location within the kidney cortex.

TABLE 2
THE FRACTION OF THE PAIRED VESSELS OBSERVED IN CROSS-SECTIONAL AREA WITH RESPECT TO THE CORTEX FRACTION

Cortex fraction (X_j)	Tissue area (mm^2)	Total number of vessels having diameter ≥0.05 mm	Paired vessels		
			Number	% of Total	per mm^2 of Tissue
0.12	115.91	264	80	30.3	0.690
0.17	127.91	185	29	15.7	0.227
0.23	148.04	287	62	21.6	0.419
0.23	141.14	303	78	25.7	0.553
0.29	112.93	169	42	24.9	0.372
0.33	108.00	208	43	20.7	0.398
0.34	102.42	153	31	20.3	0.303
0.36	172.17	175	40	22.9	0.232
0.41	87.09	59	6	10.2	0.069
0.43	141.26	177	37	20.9	0.262
0.50	166.12	192	41	21.4	0.247
0.54	128.44	104	14	13.5	0.109
0.62	115.40	91	11	12.1	0.095
0.68	157.86	100	20	20.0	0.127
0.68	140.11	120	19	15.8	0.136
0.75	172.77	139	19	13.7	0.110
0.85	178.01	106	21	19.8	0.118

increasing frequency as the cortex surface is approached. This finding was confirmed by observations made on the full-thickness longitudinal slices through the cortex. Our data support the conclusion that fewer than 31% of all the vessels within the pig kidney cortex are paired.

Prior to preparation for SEM viewing, the plastic filling the arteries appeared darker blue in color than the plastic which had passed into and filled the veins. The reason for this is unknown, but this difference made it possible to distinguish arteries from veins in both the cross- and longitudinal sections of the vascular casts. In addition to the difference in color intensity, the longitudinal views revealed differences in the pattern of branching for the arteries compared to the veins.

The branching pattern and architecture of the cortical radial arteries defined by Kriz and Bankir (1988) were studied using full-thickness longitudinal slices through the kidney cortex (approximately 13 mm, see Fig. 2b). Near the CMJ, some of the large arteries were closely accompanied by large veins. In contrast to the more or less side-by-side organization of artery–vein pairs in the deeper portions of the cortex, when pairs of vessels were observed within the outer ⅓ of the cortex, the veins were usually twisted around the arteries.

Analysis of the vascular architecture revealed in the longitudinal slices of the cortex suggest that the radial arteries give rise to about seven branching generations. Locations of the branching generations, their ranges, and standard deviations are shown in Table 3. Examination of the longitudinal slices indicate that in most situations each parent vessel branched into two daughter vessels. Branching patterns range from symmetrical, i.e., with both daughters having equal diameters,

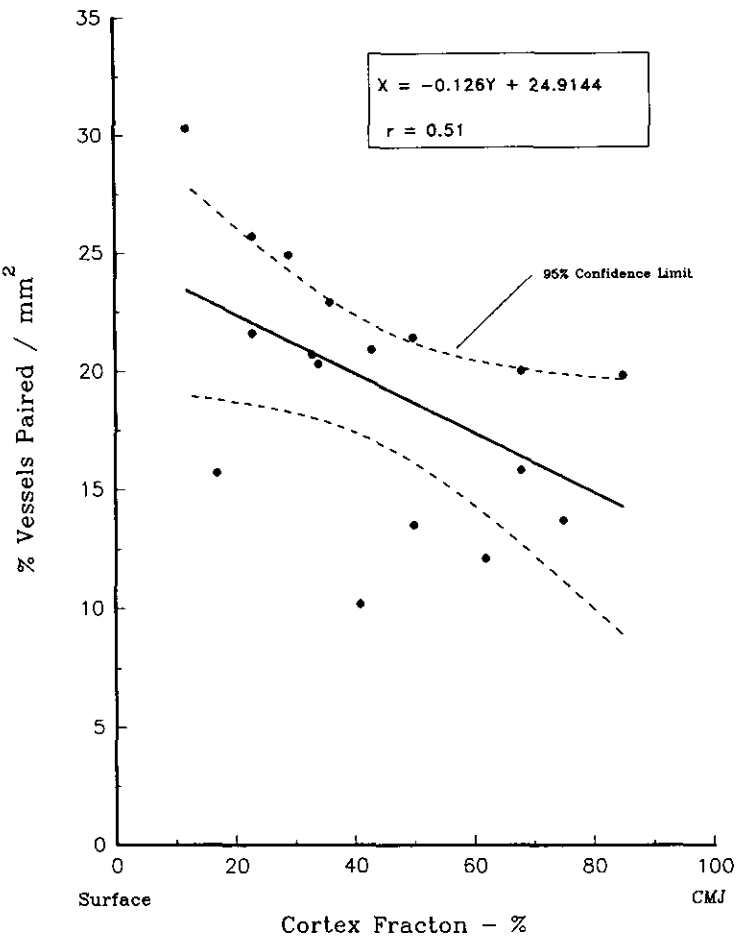

FIG. 6. The linear relationship between the paired vessel percentage per square millimeter and the cortex fraction.

TABLE 3

LOCATION AND PARENT VESSEL DIAMETER OF THE SEVEN VASCULAR BRANCHING GENERATIONS WITHIN THE PIG KIDNEY CORTEX

	Generation	Cortex fraction (%)	Vessel diameter (μm)	*n*
Surface ↑	7th	7.1 ± 1.2	39.5 ± 8.2	15
	6th	12.7 ± 1.4	101.1 ± 25.6	32
	5th	25.2 ± 6.0	138.9 ± 40.4	36
	4th	34.2 ± 5.8	200.8 ± 51.7	14
	3rd	46.9 ± 6.6	249.6 ± 63.7	17
	2nd	64.2 ± 6.2	340.9 ± 78.7	7
CMJ ↓	1st	94.6 ± 3.2	501.4 ± 90.2	4

Note. X_j is the cortex fraction, expressed as a percentage of the total cortex thickness; *n*, number of vessel (mean ± SD).

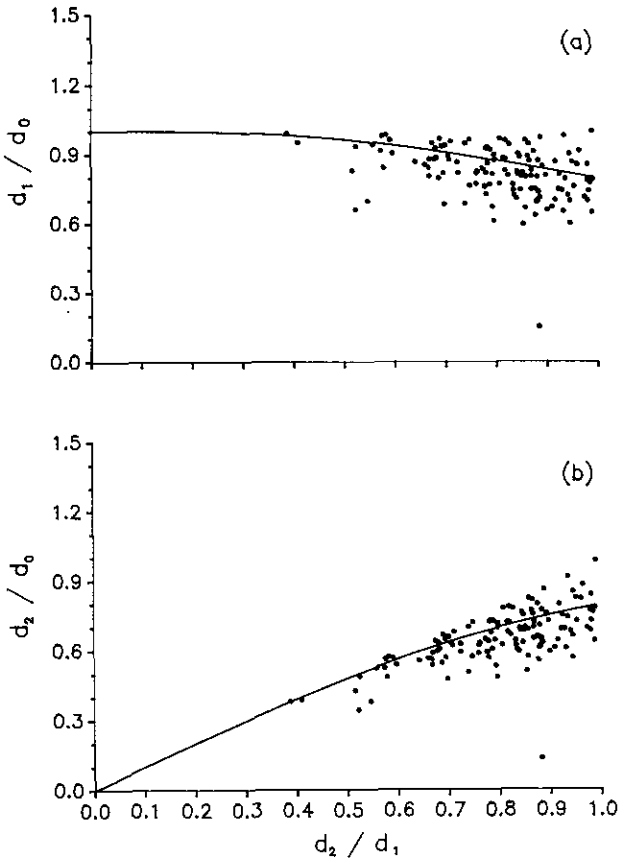

FIG. 7. Measured ratios of the daughter and parent vessel diameters, d_1/d_0 (a), d_2/d_0 (b) vs the daughter vessel diameter ratio (d_2/d_1). d_1, d_2, d_0 are the diameters of larger daughter, smaller daughter, and parent vessel, respectively. The solid lines in both (a) and (b) represent the optimal ratios.

to the rarely found situation where one of the daughters essentially maintains the size and direction of the parent while the other, much smaller one, assumes the position of a side branch. Although the branching angle as a three-dimensional quantity could not be measured using the present technique, their two-dimensional projections seen on the SEM montages were studied qualitatively. Using the digitizing tablet and software, each branching angle was estimated by first establishing a reference cursor line in the direction of the longitudinal axis of the parent vessel, then rotating it about the branching point so as to align the cursor with the axis of first one, and subsequently the other of the two branches. In general, when daughter vessels are equal in diameter they were found to branch at about equal angles from the parent vessel. When daughter vessels differ in diameter, the larger vessel consistently has a smaller branching angle and vice versa. Similar patterns have been reported for the major vessels (diameter >0.5 mm) in the rat kidney (Zamir and Phipps, 1987).

At each bifurcation, the diameters of the parent (d_0) and the daughter branches (d_1, larger; d_2, smaller) were also measured. The relationships among the ratios d_1/d_0, d_2/d_0, and d_2/d_1 at bifurcations, are shown in Fig. 7. Solid lines represent

calculated theoretical optimal ratios of daughter to parent vessel diameters, based on principles proposed by Murray (1926a,b) for minimum shear stress and minimum lumen volume at bifurcations as

$$d_1/d_0 = 1 / (1 + (d_2/d_1)^{3/2})^{1/3} \quad (1)$$

$$d_2/d_0 = (d_2/d_1) / (1 + d_2/d_1)^{3/2})^{1/3}. \quad (2)$$

Although the data are somewhat scattered, the measured parameters of the vascular geometry in the pig kidney cortex fit reasonably well to the proposed theoretical optimum.

Of the 125 bifurcations studied here, the ratio of small to large daughter branch diameters (d_2/d_1) was 0.802 ± 0.011 (mean ± SE), a value that compares favorably to 0.785 found in the pulmonary arterial tree (Horsfield and Woldenberg, 1989). The average value of the daughter/parent vessel lumen area ratio ($\beta = (d_1^2 + d_2^2)/d_0^2$) in the present study is 1.117 ± 0.024(SE). A β of 1.062 and 1.212 has been reported for the rat coronary (Zamir *et al.*, 1984) and renal artery (Zamir and Phipps, 1987) networks, respectively, and 1.0879 for the human pulmonary arterial tree (Horsfield and Woldenberg, 1989), suggesting that vascular branching patterns may be similar across organs and species. Moreover, the value of β is thought to be useful in the analysis of endothelial shear stress caused by flowing blood (Rodbord, 1975; Zamir, 1977). Shear stress has been implicated as a factor contributing to vascular disease (Fry, 1968).

Our results provide a quantitative image for the microvasculature within the pig kidney cortex. One application of these data is to estimate the average volumetric arterial blood supply passing through a cross-sectional tissue area (A_j; mm^2) at any depth within the cortex. Dividing the volumetric flow rate (mm^3/s) by the cross-sectional area yields the average blood flow velocity v_j (mm/s), generally expressed as:

$$v_j = K \cdot \omega \cdot \sum^{i} \left(\frac{VND_{ij}}{2} \cdot d_i^Z \right). \quad (3)$$

In the present study, tissue blood perfusion ω (ml/ml/s) is assumed to be uniform and constant within the kidney cortex, and measurements of vessel number density within a specific vessel diameter range (represented by d_i) at the cortex depth j (VND_{ij}; refer to Table 1). As noted previously, the vessel number density reflects a number of both arteries and veins passing through each unit cross-sectional area. We assume here that there are equal numbers of arteries and veins, and thus, in Eq (3), $VND_{ij}/2$ is the number of arteries per unit area at a given depth within the cortex. The exponent Z and the constant K are two empirically determined parameters.

The schematic drawing in Fig. 8 depicts a segment cut from the kidney cortex. In this segment, V_j represents the volume of the cortex above the plane of section A_j; and all of the blood supplying to V_j passes through A_j and flows at velocity v_j. Thus,

$$v_j = \omega \cdot V_j/A_j. \quad (4)$$

Here, the cortex cut is approximated as a segment of two concentric cylinders of

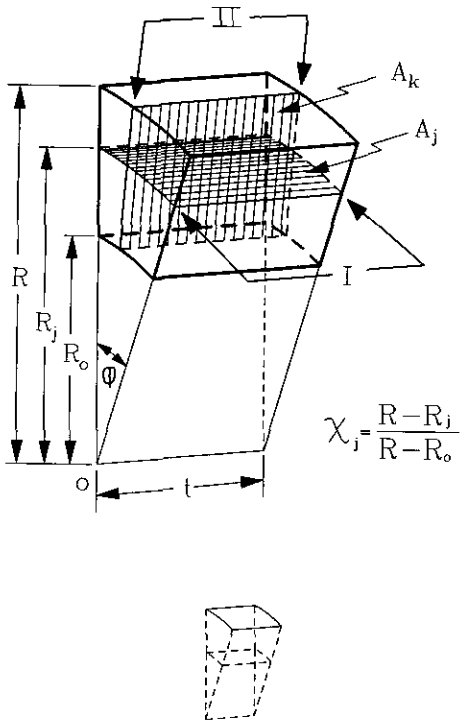

FIG. 8. Schematic drawing of a segment cut from the kidney cortex. I and II denote the directions of cutting to obtain cross (A_j) and longitudinal (A_k) sections, respectively. X_j is defined as the cortex fraction, where R, R_j, and R_c are radii from the imaginary cylindrical ring center "o" to the kidney surface, A_j and CMJ, respectively.

thickness t, outer radius R, and inner radius R_c (see Fig. 8), and the volume V_j at any radius R_j is estimated by

$$V_j = 0.5\,\varphi\, t\,(R^2 - R_j^2), \tag{5}$$

where φ is the included angle of the cylindrical segment.
Similarly,

$$A_j = \varphi \cdot R_j \cdot t. \tag{6}$$

Substitution of Eqs. (5) and (6) into Eq. (4) yields

$$v_j = 0.5 \cdot \omega\,(R^2 - R_j^2)/R_j. \tag{7}$$

Equation (7) can be combined with Eq. (3), giving

$$(R^2 - R_i^2)/R_j = K \cdot \sum_i^{\cdot} (\mathrm{VND}_{ij} \cdot d_i^Z). \tag{8}$$

Measurements of R and R_j were made from the center ("o", see Fig. 8) of the cylindrical segment to the kidney surface and the position of the cross-sectional area A_j, respectively. Equation 8 was used to calculate iteratively K and Z by fitting the measured data into the equation. The resulting values of K and Z were 966.8 and 2.52, respectively.

To our knowledge, the significance of parameter K has received little attention, whereas the exponent Z and its value has been the subject of several theoretical and experimental studies. Uylings (1977) concluded that $Z = 2.333$ is the optimal value that minimizes the total metabolic (proportional to volume) and friction power losses for a fully turbulent flow. A similar analysis by Murray (1926a) for fully developed laminar blood flow gave the optimum value of $Z = 3.0$. Analysis of the human pulmonary arterial tree suggests a value of $Z = 2.3 \pm 0.1$ (Zamir and Phipps, 1987). A Z of 2.5 has been reported for several species of botanical trees (Murray, 1927). These results suggest that in many, diverse, branching systems, the value of Z most likely lies within the range of 2.3–3.0, implying that in many, perhaps most biological structures, branching occurs in a certain universal optimal way to minimize stress within the system.

In view of recent attempts to offer a more precise understanding of heat transfer mechanisms in living tissues (Baish *et al.*, 1986; Chen and Holmes, 1980; Weinbaum *et al.*, 1984), it has become increasingly important to gain detailed information regarding the microvasculature of vessels having significant contribution to heat transfer in local tissue. These vessels normally have diameters within the range of approximately 0.05 to 0.5 mm. The present work offers a quantitative image of them within the pig renal cortex and the findings should provide an important foundation for heat transfer studies in the future.

ACKNOWLEDGMENTS

The research in this paper was supported in part by NIH-NHLBI Grant HL 27011. The authors express their sincere thanks to the Center for Electron Microscopy at University of Illinois for the use, without cost, of the ISI-130 scanning electron microscope. We also thank Drs. Thomas Adams and John Chato for their thoughtful editorial comments and suggestions. Our appreciation is extended to Ms. Kathleen VonRuff for help with the data collection.

NOMENCLATURE

A	cross-sectional area, [mm^2]
a	distance between centers of the two paired vessels, [mm]
CMJ	corticomedullary junction
d	vessel diameter, [mm]
K	empirical constant in equation (3)
R	distance between a cross-section and a center of an imaginary cylindrical ring (see Fig. 1), [mm]
SEM	Scanning Electron Microscope
t	thickness of a segment cut from the kidney cortex (see Fig. 1), [mm]
TVND	total vessel number density = the total number of vessels (d $\geqslant$ 0.05mm) transversing a unit cross-sectional area of the kidney cortex, [#/mm^2]
v	average blood flux, [mm/s]
V	partial volume of a segment cut from the kidney cortex (see equation (5)) [mm^3]
VAF	cross-sectional vessel area fraction (vessel area / tissue area)

VND	vessel number density = the number of vessels with specific diameter transversing a unit cross-sectional area of the kidney cortex, [#/mm^2]
X	cortex fraction: the ratio of the depth of a given cross section from the surface and the thickness of the kidney cortex (see Fig. 1)
Z	empirical exponent in equation (3)
Greek letters	
β	lumen area ratio of daughters to parent vessel, defined as $\beta = (d_1^2 + d_2^2)/d_0^2$
ω	blood perfusion rate, [ml/ml/s]
φ	included angle of a segment cut from kidney cortex [radian]
Subscripts	
c	at the corticomedullary junction
i	index of the range of vessel diameters
j	index of the cortex fraction
o	at the center of an imaginary cylindrical ring in Fig. 1
0	parent vessel
1	large daughter vessel
2	small daughter vessel

REFERENCES

BAISH, J. W., AYYASWAMY, P. S. AND FOSTER, K. R. (1986a). Small-scale temperature fluctuations in perfused tissue during local hyperthermia. *ASME J. Biomech. Eng.* **108,** 246–250.

BAISH, J. W., AYYASWAMY, P. S., AND FOSTER, K. R. (1986b). Heat transport mechanisms in vascular tissues: A model comparison. *ASME J. Biomech. Eng.* **108,** 324–331.

BENKESER, P. J., FRIZZELL, L. A., HOLMES, K. R., AND GOSS, S. A. (1990). A perfused tissue phantom for ultrasound hyperthermia. *IEEE Trans. Biomed. Eng.* **37,** 425–428.

CHATO, J. C. (1991). Fundamentals of bioheat transfer. *In* Thermal Dosimetry and Treatment Planning (M. Gautherie, Ed.). Springer-Verlag.

CHEN, M. M., AND HOLMES, K. R. (1980). Microvascular contributions in tissue heat transfer. *Ann. NY Acad. Sci.* **335,** 137–150.

DAGAN, Z., WEINBAUM, S., AND JIJI, L. M. (1986). Parametric studies on the three-layer microcirculatory model for surface tissue energy exchange. *ASME J. Biomech. Eng.* **108,** 89–96.

FRY, D. L. (1968). Acute vascular endothelial changes associated with increased blood velocity. *Circ. Res.* **22,** 165–197.

HORSFIELD, K., AND WOLDENBERG, M. J. (1989). Diameters and cross-sectional areas of branches in the human pulmonary arterial tree. *Anatom. Rec.* **223,** 245–251.

KRIZ, W., AND BANKIR, L. (1988). A standard nomenclature for structures of the kidney. *Am. J. Physiol.* **254,** F1–F8.

LEMONS, D. E., CHIEN, S., CRAWSHAW, L. I., WEINBAUM, S., AND JIJI, L. M. (1987). Significance Of vessel size and type in vascular heat transfer. *Am. J. Physiol.* **253,** R128–R135.

MOORE, B. J., HOLMES, K. R., AND XU, L. X. (1992). Vascular anatomy of the pig kidney glomerulus: A qualitative study of corrosion casts. *Scanning Microsc.* **6,** 887–898.

MURRAY, C. D. (1926a). The physiological principle of minimum work applied to the angle of branching of arteries, *J. Gen. Phys.* **9,** 835–841.

MURRAY, C. D. (1926b). The physiological principle of minimum work. I. The vascular system and the cost of blood volume, *Proc. Nat. Acad. Sci. USA* **12,** 207–214.

MURRAY, C. D. (1927). A relationship between circumference and weight in trees and its bearing on branching angles. *J. Gen. Physiol.* **10,** 725–729.

RODBORD, S. (1975). Vascular caliber. *Cardiology* **60,** 4–49.

UMEMURA, S. I., HOLMES, K. R., FRIZZELL, L. A., AND CAIN, C. A. (1992). Insonation of fixed porcine kidney by a prototype sector-vortex-phased array applicator. *Int. J. Hyperthermia* **8**(6), 831–842.

UYLINGS, H. B. M. (1977). Optimization of diameters and bifurcation angles in lung and vascular tree structures. *Bull. Math. Biol.* **39,** 509–520.

WEINBAUM, S., JIJI, L. M., AND LEMONS, D. E. (1984). Theory and experiment for the effect of vascular temperature on surface tissue heat transfer. I. Anatomical foundation and model conceptualization. ASME *J. Biomech. Eng.* **108,** 321–330.

ZAMIR, M. (1977). Shear forces and blood vessel radii in the cardiovascular system. *J. Gen. Physiol.* **69,** 449–461.

ZAMIR, M., PHIPPS, S., LANGILE, B. L., AND WONNACOTT, T. H. (1984). Branching characteristics of coronary arteries in rats. *Can. J. Physiol. Pharmacol.* **62,** 1453–1459.

ZAMIR, M., AND PHIPPS, S. (1987). Morphometric analysis of the distributing vessels of the kidney. *Can. J. Physiol. Pharmacol.* **65,** 2433–2440.